

Cardiac mapping of electrical impedance tomography by means of a wavelet model

Harki Tanaka¹, Neli Regina Siqueira Ortega², Andre Hovnanian³,
Carlos Roberto Ribeiro de Carvalho³, Marcelo Britto Passos Amato³

¹Center of Engineering, Modelling and Applied Social Sciences, Federal University of ABC, São Paulo, Brazil

²Center of Fuzzy Systems in Health, School of Medicine, University of São Paulo, São Paulo, Brazil

³Respiratory Intensive Care Unit, Hospital das Clínicas, School of Medicine, University of São Paulo, São Paulo, Brazil

Email: harki.tanaka@gmail.com

Received 25 July 2013; revised 26 August 2013; accepted 14 September 2013

Copyright © 2013 Harki Tanaka *et al.* This is an open access article distributed under the Creative Commons Attribution License, which permits unrestricted use, distribution, and reproduction in any medium, provided the original work is properly cited.

ABSTRACT

To improve the identification of cardiac regions in Electrical impedance tomography (EIT) pulmonary perfusion images, a model of wavelet transform was developed. The main goal was to generate maps of the heart using EIT images in a controlled animal experiment using a healthy pig and in two human volunteers. The model was capable of identifying the heart regions, demonstrated robustness and generated satisfactory results. The pig images were compared to perfusion images obtained using injection of a hypertonic solution and achieved an average area of the ROC curve of 0.88. The human images were qualitatively compared with Computerized Tomography scan (CT-scan) images.

Keywords: Electrical Impedance Tomography; Heart; Image Analysis; Image Segmentation; Wavelet

1. INTRODUCTION

Electrical impedance tomography EIT is an imaging technique, still in development, in which an image of the conductivity of a transverse section of an object is inferred from electrical measurements performed using a series of electrodes placed on its surface [1,2]. Despite its benefits, the method has a major drawback, as its low spatial resolution hinders the characterization of the activity of regions according to their physiological origin in a dynamic image. This difficulty in the interpretation of images can be translated as an uncertainty in the identification of pixels in both anatomical and functional terms. Important EIT studies focus on the acquisition and interpretation of thoracic images. During the cardio-respiratory cycle, air and blood share the same compartment

and rhythmically change their volumes. Thus one major application of EIT is the monitoring of cardio-respiratory functioning [3-8]. The EIT method has several benefits: it is a non-invasive method with no harmful radiation, has a high temporal resolution and low cost, and allows for the bedside monitoring of a patient [6]. The low spatial resolution of EIT images remains an unsolved problem and provides opportunities for new approaches to improve EIT imaging applications [6]. Low spatial resolution can be addressed through improvements in the image construction algorithm [6-9] and through the development of systems based on post-constructed images using dynamical and physiological information. There are many techniques for the analysis of biomedical signals. One of the most common is the Fourier transform. However, despite its vast applicability, the Fourier transform is not able to provide a time-frequency representation of the signals, which is important in the analysis of non-stationary signals [10]. The wavelet transform is emerged as a tool to overcome this limitation [11,12]. In this work, a new methodology was proposed to improve the spatial resolution of EIT images of pulmonary perfusion based on wavelet transform.

2. METHODS

To develop a methodology capable of identifying the heart region in EIT images, a qualitative analysis of bio-impedance waveforms was performed. In this qualitative analysis, each pixel signal was grouped into characteristic regions based on the signal's waveform patterns. These grouped patterns were discussed with a panel of experts, taking into account the physiological knowledge of cardio-respiratory dynamics. This qualitative analysis provided the characteristic behavior of each region of the chest used in the algorithm development. The model was

developed based on the collected animal experimental data and evaluated using both the animal and human EIT data. This study was approved by the Research Ethics Committee of the School of Medicine of São Paulo University (protocol number 0832/07), and subjects gave informed consent to the work.

2.1. Data Collection

In this work, four data sets were used:

- 1) EIT perfusion data extracted from one healthy male pig, called P1, used for wavelet method development;
- 2) EIT saline data extracted from the same pig used as the EIT reference image;
- 3) EIT perfusion data extracted from two healthy male humans, called H₁ and H₂, used for the evaluation of the developed method; and
- 4) CT-scan images obtained from both men used as reference thoracic images.

2.1.1. EIT Data Acquisition in an Animal Experiment

EIT data were collected using the Enlight[®] (Timpel SA, Sao Paulo, Brazil). The electrical current used in the electrodes was 5 mA at 125 KHz. Each EIT image consisted of a matrix of 32 × 32 pixels and was acquired at an image acquisition rate of 50 frames per second. An ECG-gated image set was generated to represent the cardiac cycle and was synchronized with the peak of the R-wave of the ECG signal [6]. The wavelet transform was applied to the EIT signals of perfusion images, obtained by means of the ECG-gated temporal averaging of the EIT raw data. During the experiment, the pig was submitted to mechanical ventilation assistance, and three positive end-expiratory pressure (PEEP) ventilation parameters were used: 18 cm H₂O (PEEP18), 12 cm H₂O (PEEP12) and 0 cm H₂O (ZEEP). For each PEEP value, 5 ml of a hypertonic solution (20% NaCl) was injected through a catheter into the right atrium of the pig during apnea [6]. Saline was used as a contrast agent for EIT imaging [13] and allowed for mapping of cardiovascular regions. This experiment has been previously described in full in [6].

2.1.2. EIT Data Acquisition in Human Subjects

The same EIT tomography based on the Enlight[®] technology was used to collect EIT data of the human thorax. The data were collected from two volunteers, and in both subjects, the EIT data were acquired with ECG signals. Volunteer H₁ was placed in a supine rest position, and thirty-two electrodes were placed circumferentially and equally spaced around the thorax at three positions (**Figure 1**): high level—the great vessels, aorta and pulmonary artery; medium level—the transition area between the region of the great vessels and the ventricles; and low level—the ventricles region. Therefore, three sets of EIT



Figure 1. Thirty-two electrodes were placed circumferentially and equally spaced around the human thorax at three positions.

raw data were collected. The volunteer H₂ was placed in two positions: a supine rest position and a sitting rest position.

Thirty-two electrodes were placed circumferentially and equally spaced around the thorax at the level of the cardiac chambers, and two sets EIT raw data were collected.

2.1.3. Computed Tomography (CT) Image Acquisition in Human Subjects

A 16-channel X-ray CT (Angio CT, General Electric[™]) was used to generate cross-sectional images of the thorax. These thoracic images were obtained from the same volunteers that were submitted to EIT data collection. The volunteers were healthy; one (H₁) was 32 years old, and the other (H₂) was 29 years old. CT angiography of pulmonary arteries was performed with an injection of 15 mL X-ray contrast into the right antecubital vein. The image acquisition was performed at the same level as the EIT electrodes band.

2.2. Model Elaboration

Model development was based on the EIT images of pulmonary perfusion obtained in the animal experiment under PEEP18. The images acquired at PEEP12 and ZEEP were used to improve the method. This multistep evaluation was important to evaluate the robustness of the system.

2.2.1. Qualitative Analysis of EIT Temporal Signals Patterns

Images of one cardiac cycle were produced from the collected pig thorax data with controlled pressure PEEP18 using a coherent mean method [6]. Qualitative analysis

of the EIT temporal signals of the pixels was performed to identify macro regions according to the observed variations in bio-impedance during the cardiac cycle. To identify the regions with similar signals, a qualitative evaluation of the signal patterns was performed. Following this qualitative analysis, the pixels were grouped into regions based on similarities in their dynamic behaviors, and a characteristic pixel for each region was chosen. After the identification of the regions and their characteristic signals, each signal was analyzed by qualitatively comparing the variation of impedance with the variation of blood flow during the cardiac cycle. Based on the experience of experts in the respiratory ICU at the Clinics Hospital of São Paulo, Brazil, in a consensus method, we decided whether each pixel more likely belonged to the heart or lungs. This analysis required that the beginning of each EIT signal was synchronized with the peak of the R-wave of the ECG signal, marking the beginning of systole, *i.e.*, ventricular contraction.

2.2.2. Wavelet Methods for Identification of Cardiac Regions

From the qualitative analysis, it was assumed that a typical pixel within the cardiac region has a positive variation in impedance during the first half of the cardiac cycle. Thus, for a set of images of a complete cardiac cycle, the pixel with the highest increase in impedance was selected. This pixel was considered to be the best representation of the cardiac region, and the analysis of all other pixels was conducted relative to the reference pixel. A wavelet transform was applied to the impedance signal of the reference pixel using as wavelet-mother the *gaus4* to obtain the space of coefficients in the plane dislocation-scale. The values of these coefficients were normalized to the interval [0,1]. After normalization, a threshold of 0.70 was applied to define a region in the dislocation-scale space that reflected typical cardiac behavior. This region was used as a mask in the dislocation-scale space to compare all pixels with the reference pixel. For each pixel, the same processes of the wavelet transform and the normalization of the space coefficients were performed. The reference mask was applied to each of the displacement-scale spaces and a set of coefficient values was selected. This set of coefficients was used to determine whether each pixel belonged in the cardiac region. Using these values, it was possible to create a map of parameters representing all pixels. In this study, two possible parameters were analyzed: the average values of the coefficients of the mask (method-1); and the maximum value of the coefficients of the mask (method-2). The cardiac images were generated from a z-score normalization on the parameter map. In this normalized space, a threshold value for a pixel belonging to the cardiac region can be heuristically established.

In this case, a threshold value of 0.5 was used.

2.3. Model Evaluation

To evaluate its performance, the model was used to analyze EIT images from the animal experiment collected at other values of PEEP. In this analysis, the cardiac regions obtained by the saline injection method were used as a reference for comparison, and the system performance was evaluated using receiver operating characteristic (ROC) curves. It is important to highlight that the saline injection image is not the gold standard for imaging of the heart region. When we compare the results of the model with the saline data, we are only verifying how well the model reproduces the contrast data. As saline images are not feasible for human subjects, it was not possible to evaluate the system using ROC curves. Therefore, the EIT images of the heart region in humans were qualitatively compared with X-ray CT images.

3. RESULTS

3.1. The Dynamics of the EIT Signal Carry Information That Allows for Pixel Characterization as Belonging to the Cardiac Region

Through qualitative analysis of the EIT signal patterns, a map was generated in which the pixels were grouped based on their similarities (Figure 2). Tables 1 and 2 show the qualitative analysis, describe the characteristics of each region and link them to their possible anatomical regions. In Table 1, pixel 214 shows a typical variation in impedance of the ventricular region during the cardiac cycle, and pixel 630 shows a typical variation of impedance of a pulmonary region.

Table 2 presents examples of pixels where the impedance variation is not typical of either heart or lung re-

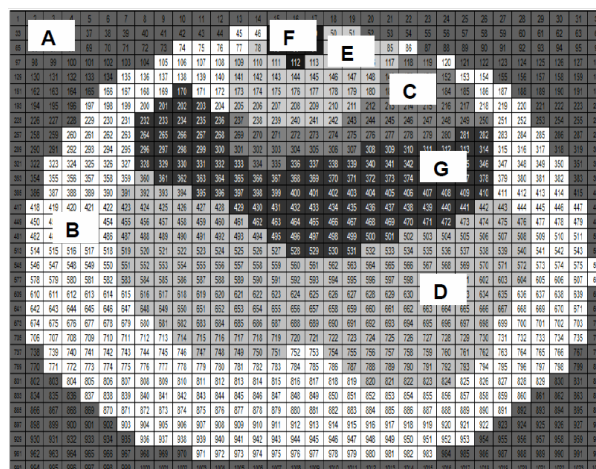
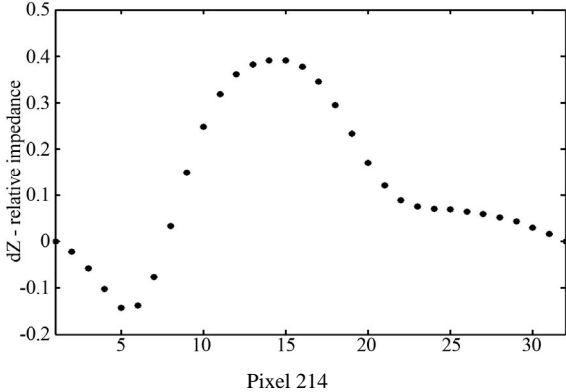
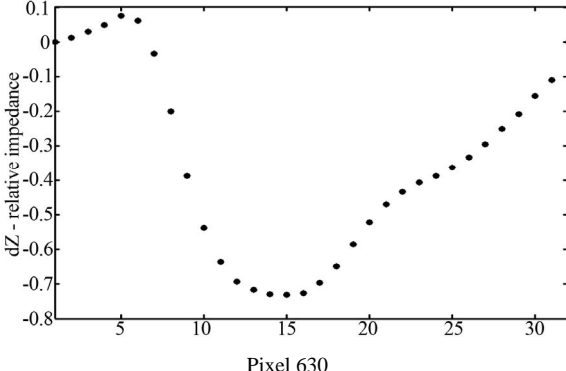


Figure 2. EIT Map with the regions found by qualitative analysis of the wave patterns of a pig's EIT signals.

Table 1. Qualitative map and the characteristic EIT signals-regions A, B, C and D.

Regions	Characteristic signal	Analysis	Pixel hypothesis
A	-	Region out of analysis.	-
B	-	Pixels without significant impedance variation ($dZ < 0.1$).	-
C		1-32: full cardiac cycle. 1-5: impedance decrease during the atrial systole. 5-6: isovolumetric contraction of systolic phase. 6-16: Ventricular systole. 6-11: systolic phase—rapid ejection. 11-15: systolic phase—reduced ejection. 15-16: systolic phase—iso-volumetric relaxation. 16-32: diastolic phase. 16-22: diastolic phase rapid filling. 22-32: diastolic phase reduced filling.	Pixel of cardiac region (ventricle)
D		The impedance variation is opposite to that observed in the previous region. This behavior is expected in the pulmonary region because of the pulmonary circulation: the blood flow that leaves the right ventricle during the systolic phase reaches the lungs.	Pixel of pulmonary region

gions. **Figure 3** shows the pig heart maps obtained using the wavelet and saline contrast methods. Pixels corresponding to the heart region are located in a superior central position independent of the PEEP values.

3.2. The Maps Obtained Using the Cardiac Wavelet Models Are Comparable to the Maps Obtained by the Cardiac Saline Method

For comparison of the wavelet heart maps with the image of the saline cardiac region, ROC curves were elaborated for each PEEP value (**Figure 4**). The average areas of the ROC curves were 0.86 for method-1 and 0.90 for method-2, demonstrating that these methods were comparable to the saline method.

3.3. Humans Images of the Cardiac Regions Obtained by Methodology Proposed Were Qualitatively Comparable with the Angio CT images

Figure 5 shows the heart maps of the first human (H1)

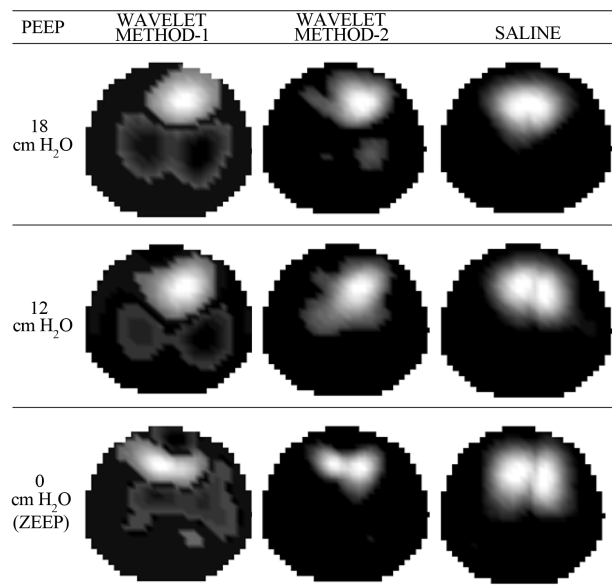


Figure 3. Pig heart maps obtained by the wavelet and saline injection methods for each PEEP value, (white color indicates the cardiac region).

Table 2. Qualitative map and the characteristic EIT signals-regions E, F and G.

Regions	Characteristic signal	Analysis	Pixel hypothesis
E		<p>1-21: impedance variation similar to systolic phase as in region C. 21-32: different pattern if compared to regions C and D.</p>	Pixel of predominantly cardiac region
F		<p>1-21: impedance variation similar to systolic phase as in region C. 21-32: different pattern if compared to regions C and D.</p>	Pixel possibly of cardiac region
G		<p>1-16: impedance variation similar to systolic phase as in region D. 16-32 different pattern if compared to regions C and D.</p>	Pixel of predominantly pulmonary region

obtained using the wavelet methods and the Angio CT images for three positions of the electrodes belt. The two wavelet methods were able to identify the cardiac region regardless of the position of the electrode belt.

These regions are qualitatively consistent with the Angio CT images. **Figure 6** shows the heart maps of the second human (H2) obtained using the wavelet methods and the Angio CT images. Both methods were able to identify the cardiac region regardless of the body position. In this case, the images obtained using method-1 were more similar to the Angio CT images than those obtained using method-2.

4. DISCUSSION

Two wavelet methods were developed to identify the cardiac region of a pig submitted to three different values of PEEP. Both methods demonstrated adequate quantitative and qualitative results. The best results were obtained at the pressure PEEP12, followed by PEEP18 and finally by ZEEP. One possible hypothesis for this observation is that variations in the PEEP value may modify the position of the band of thirty two electrodes in the cranial-caudal direction, and therefore, the transverse section that covers the heart. Based on this as sumption, the pressure PEEP12 favored the identification of the

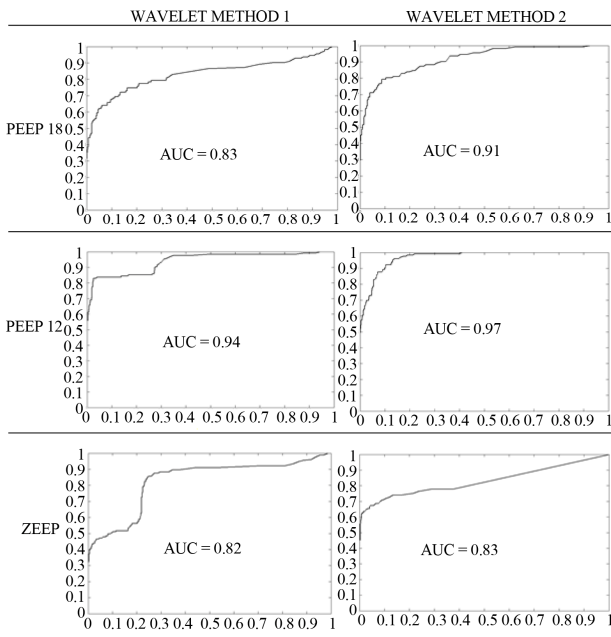


Figure 4. ROC curves obtained using the wavelet methods compared with the pig heart region obtained through a saline injection for each PEEP value.

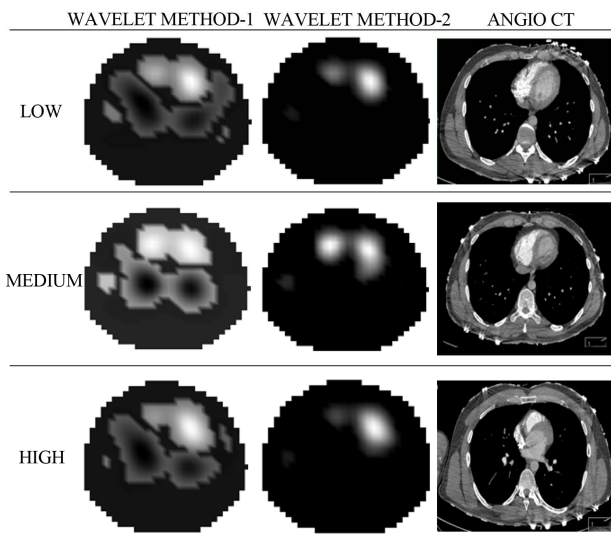


Figure 5. Human (H1) heart maps obtained by the wavelet methods for each position of the band of 32-electrodes and the corresponding Angio CT images (white color indicates the cardiac region).

cardiac region because extremes of PEEP can result in the augmentation in pulmonary vascular resistance and compromise of right ventricular function. The wavelet methods were applied to two human EIT images and the models were able to adequately identify the heart in both cases. These results are in accordance with the assumption that the hearts of pigs and humans are very similar anatomically and functionally [14].

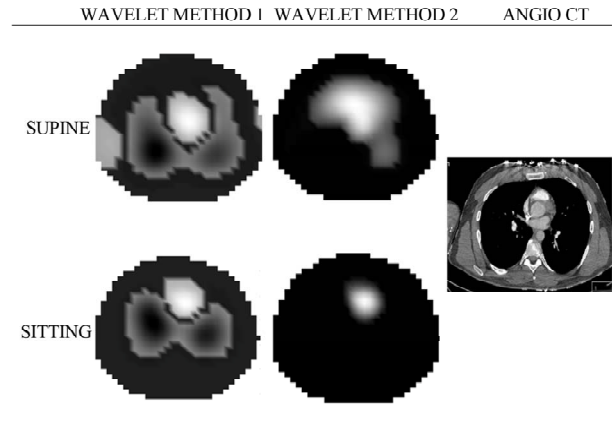


Figure 6. Human (H2) heart maps obtained by the wavelet methods for the two body positions of the subject and the corresponding Angio CT image (white color indicates the cardiac region).

Comparing the two methods, lung perfusion imaging was observed in images acquired with method-1 but not in images obtained with method-2. The main difference between the approaches is the choice of parameter mapping pixels. In the first method, the average value of the coefficients was used, and in the second method, the maximum value of the coefficients was used. Therefore, a more pronounced difference between the parameters is expected when using method-2, which produces a crisper image. In conclusion, the wavelet method discussed here is a feasible means of analysis for EIT imaging, which is a research area to be explored. Methods presented in this study may be used in two fields of analysis: 1) improvement of EIT imaging by, for example, providing a priori information for image reconstruction algorithms; and 2) assisting in the development of systems for clinical application such as the estimation of non-invasive cardiac debt.

5. ACKNOWLEDGEMENTS

We would like to acknowledge all of the experts in the respiratory ICU at the Clinics Hospital of São Paulo, Brazil who helped in the qualitative analysis of the EIT images. This work was financially supported by CNPq (484116/2007-0).

REFERENCES

- [1] Adler, A., Amyot, R., Guardo, R., Bates, J.H.T. and Berthiaume, Y. (1997) Monitoring changes in lung air and liquid volumes with electrical impedance tomography. *Journal of Applied Physics*, **83**, 1762.
- [2] Barber, D.C. (1989) A review of image reconstruction techniques for electrical impedance tomography. *Medical Physics*, **16**, 162. <http://dx.doi.org/10.1118/1.596368>
- [3] Brown, B.H. (2003) Electrical impedance tomography (EIT): A review. *Journal of Medical Engineering & Te-*

- chnology, **27**, 97.
<http://dx.doi.org/10.1080/0309190021000059687>
- [4] Eyüboğlu, B.M., Brown, B.H. and Barber, D.C. (1989) *In vivo* imaging of cardiac related impedance changes. *IEEE Engineering in Medicine and Biology Magazine*, **8**, 39.
<http://dx.doi.org/10.1109/51.32404>
- [5] Solà, J., Adler, A., Santos, A., Tusman, G., Sipmann, F.S. and Bohm, S.H. (2011) Non-Invasive Monitoring of Central Blood Pressure by Electrical Impedance Tomography: First Experimental Evidence. *Medical & Biological Engineering & Computing*, **49**, 409.
<http://dx.doi.org/10.1007/s11517-011-0753-z>
- [6] Tanaka, H., Ortega, N.R.S., Galizia, M.S., Borges, J.B. and Amato, M.B.P. (2008) Fuzzy modeling of electrical impedance tomography images of the lungs. *Clinics*, **63**, 363.
<http://dx.doi.org/10.1590/S1807-59322008000300013>
- [7] Victorino, J.A., Borges, J.B., Okamoto, V.N., Matos, G.F.J., Tucci, M.R., Caraméz, M.P.R., Tanaka, H., Sipmann, F.S., Santos, D.C.B., Barbas, C.S.V., Carvalho, C.R.R. and Amato, M.B.P. (2004) Imbalances in regional lung ventilation: A validation study on electrical impedance tomography. *American Journal of Respiratory and Critical Care Medicine*, **169**, 791.
<http://dx.doi.org/10.1164/rccm.200301-133OC>
- [8] Teharani, J., Oh, T.I., Jin, C., Thiagalingam, A. and McEwan, A. (2012) Evaluation of different stimulation and measurement patterns based on internal electrode: Application in cardiac impedance tomography. *Computers in Biology and Medicine*, **42**, 1122.
<http://dx.doi.org/10.1016/j.combiomed.2012.09.004>
- [9] Holder, D.S. (2005) *Electrical impedance tomography: Methods, history and applications*. Institute of Physics Publishing, Bristol and Philadelphia.
- [10] Noor, J.A.E. (2007) *Electrical impedance tomography at low frequencies*. MS Thesis, University of New South Wales, Australia.
- [11] Alfaouri, M., Daqrouq, K. (2008) ECG signal denoising by wavelet transform thresholding. *American Journal of Applied Sciences*, **5**, 276.
<http://dx.doi.org/10.3844/ajassp.2008.276.281>
- [12] Hubbard, B.B. (1998) *The world according to wavelets: The story of a mathematical technique in the making*. 2nd Edition, A K Peters Ltd., Natick.
- [13] Frerichs, I., Hinz, J., Herrmann, P., Weisser, G., Hahn, G. and Quintel, M. (2002) Regional lung perfusion as determined by electrical impedance tomography in comparison with electron beam CT imaging. *IEEE Trans Med Imaging*, **21**, 646.
<http://dx.doi.org/10.1109/TMI.2002.800585>
- [14] Crick, S.J., Sheppard, M.N., Ho, S.Y., Gebstein, L. and Anderson, R. (1998) Anatomy of the pig heart: Comparisons with normal human cardiac structure. *Journal of Anatomy*, **193**, 105.
<http://dx.doi.org/10.1046/j.1469-7580.1998.19310105.x>